Centred Splash of a Vertical Jet on a Horizontal Rotating Disc: Recent Findings and Resolving Controversies Over the Hydraulic Jump

Bernhard Scheichl

Abstract Highlights of the asymptotic and numerical analysis of the steady axisymmetric swirl flow of a Newtonian liquid over a spinning disc and generated by a jet, impacting perpendicularly onto the latter in the direction of gravity, are presented. Ubiquitous in engineering applications and involving a myriad of disparate velocity and length scales, thus extreme aspect ratios, this flow configuration is an archetypic one for the application of dimensional reasoning and matched asymptotic expansions in fluid dynamics. Particular interest lies on the recent advances in the rigorous description of the thin developed layer relatively far from the jet, which is essentially parametrised by a suitably defined Rossby number, the influence of gravity on the thin film and its interplay with a finitely remote disc edge. The latter upstream influence explains the phenomenon of the hydraulic jump in developed flow. The clarification of long-standing and more recent controversies around this concludes the analysis.

1 Origin and Statement of the Problem

Thin liquid films, involving the hydraulic jump as an important phenomenon, are ubiquitous in fluids engineering. The axisymmetric non-rotating jump can be reproduced readily in a kitchen sink. From the viewpoint of applications, however, the flow over a rotating disc attracts even more interest. This we study asymptotically.

In the following, we tacitly refer to the sketch of the assumed flow configuration in Fig. 1 and the subsequent assumptions. The horizontal and vertical direc-

Bernhard Scheichl

Institute of Fluid Mechanics and Heat Transfer, Technische Universität Wien, Tower BA/E322, Getreidemarkt 9, 1060 Vienna, Austria, e-mail: bernhard.scheichl@tuwien.ac.at

AC2T research GmbH (Austrian Excellence Center for Tribology), Viktor-Kaplan-Straße 2/C, 2700 Wiener Neustadt, Austria, e-mail: bernhard.scheichl@ac2t.ac.at

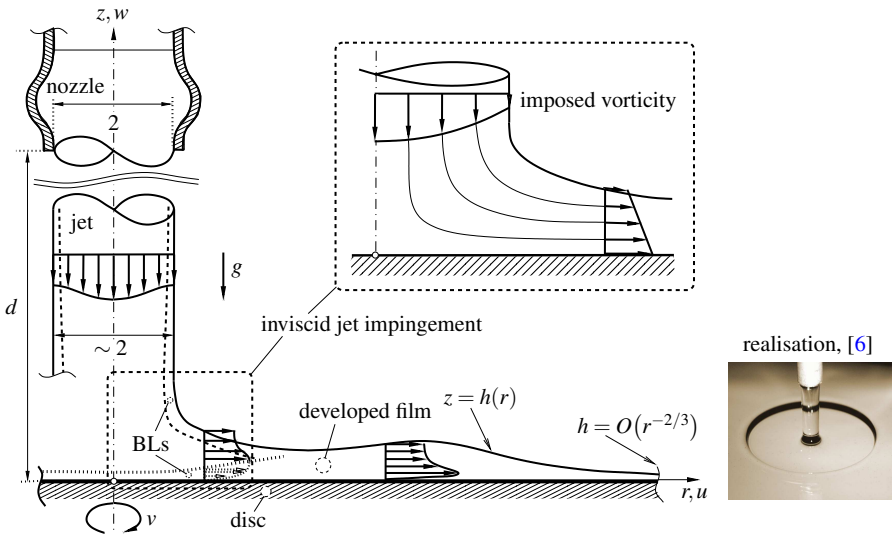

Fig. 1 Viable flow configuration for generating a radially spreading liquid film (not to scale, quantities non-dimensional), realisation exhibiting a strong hydraulic jump (taken from [6], reprinted with permission)

tions are given by respectively the plane aligned with a rigid, impervious, perfectly smooth disc and its axis of rotation. This coincides with that of a liquid jet with circular cross-section and exiting a nozzle, positioned sufficiently far above the disc, as driven by gravity acting vertically. The liquid is a Newtonian fluid of uniform density, (kinematic) viscosity, and surface tension with respect to the gaseous environment at rest and under constant pressure. Its so generated fluid flow past the disc is stationary (laminar) and axisymmetric throughout. Two radii come in the shortlist as reference lengths for the flow: that of the nozzle, typical of the jet unperturbed by its impingement, and the radius of the disc defining its edge. Since the second is only of concern if elliptic effects are, i.e. the upstream influence by gravity and/or surface tension, the first is preferred. The cross-section-averaged flow velocity at the nozzle exit then serves as the reference flow speed, and all variables are non-dimensional accordingly; subscripts indicate (unambiguously) partial derivatives.

We introduce polar coordinates r, z in respectively the radial and vertical directions, having their origin in the disc centre where the flow stagnates, and the dependent quantities $[u,v,w,p](r,z)$ and $h(r)$ denoting the radial, azimuthal, and vertical flow components, the difference p of the pressure in the fluid and the gaseous environment, and the (in case of jet contraction by gravity, double-valued) vertical height of the liquid layer respectively. Then the key groups

$$d \gg 1, \quad r_e \gg 1, \quad \nu \ll 1, \quad g \ll 1, \quad \sigma \ll 1, \quad 0 \leq \alpha_0 < \infty \qquad \text{(1a–f)}$$

essentially parametrise the flow. Herein, $z = d$ and $r = r_e$ indicate the positions of the nozzle orifice and the disc edge, and the other quantities denote reciprocal

Reynolds, Froude, and Weber numbers and a reciprocal squared Rossby number respectively (in the order of their appearance). The insinuated asymptotic limits are corroborated by the definitions of these quantities and the range of values they usually assume in engineering practice. In addition, we require ν to satisfy the sharper constraint

$$\nu d \ll 1. \tag{2}$$

We also note that the well-known Rayleigh–Plateau instability is safely avoided, thus the jet sufficiently smooth and stable, as long as d^2 is sufficiently large as compared to the Weber number $1/\sigma$.

The Navier–Stokes equations governing this free-surface flow comprise the continuity equation satisfied identically by a streamfunction ψ,

$$r[u,w] = [\psi_z, -\psi_r], \tag{3}$$

and the momentum equations for the r-, azimuthal, and z-directions respectively,

$$uu_r + wu_z - v^2/r = \nu\{[(ru)_r/r]_r + u_{zz}\} - p_r, \tag{4}$$
$$uv_r + wv_z + uv/r = \nu\{[(rv)_r/r]_r + v_{zz}\}, \tag{5}$$
$$uw_r + ww_z = \nu\{(rw_r)_r/r + w_{zz}\} - p_z - g. \tag{6}$$

The third contributions to in (4) and (5) are the centripetal and Coriolis acceleration in the Eulerian frame. Usual boundary conditions (BCs) account for axial symmetry, no-penetration of and no-slip on the disc, and conservation of the volume flow rate

$$r = 0\colon\ \psi = w_r = 0, \quad z = 0\colon\ \psi = u = 0,\ v = \sqrt{\alpha_0}\, r, \quad z = h(r)\colon\ \psi = \tfrac{1}{2}. \tag{7a–d}$$

Having in mind Bonnet's expression for the mean curvature κ of the free surface of the liquid, $\kappa = -(2r)^{-1}\,\mathrm{d}\big[rh'(1+h'^2)^{-1/2}\big]/\mathrm{d}r$, we arrive at the additional dynamic BCs holding at the latter,

$$[2h'(w_z - u_r) + (1-h'^2)(u_z + w_r)]_{z=h} = 0, \tag{8}$$
$$[v_z - h'(v_r - v/r)]_{z=h} = 0, \tag{9}$$
$$2\nu[h'^2 u_r - h'(u_z + w_r) + w_z]_{z=h} = (1+h'^2)(p|_{z=h} - 2\sigma\kappa). \tag{10}$$

These express vanishing total stress components in respectively the median, azimuthal, and surface-normal directions. The first two represent free-slip conditions, the latter takes into account the capillary (Laplace) pressure jump. Finally, the appropriate upstream or initial conditions (ICs) and downstream conditions then read

$$[\psi, u, v, w, p](r,d) = [\psi_o(r), 0, 0, -\psi_o'/r, \sigma], \quad h(1) = d, \quad h(r_e) = h_e. \tag{11a–c}$$

Here $\psi_o(r)$ subject to (7d) *models* the flow profile at the nozzle outlet, where the pressure is given by the capillary hoop stress in agreement with (10); prescribing a film height h_e at the disc edge, however, must be reviewed critically: see Sect. 3.

For a more elaborate discussion of the set of the full governing equations (1)–(11) we refer to the forerunner study [7]. The present one revisits its essence, focusses on some interesting intricacies of the analysis therein, and is intended to represent its supplement and a noteworthy extension. Specifically, the reader is provided with a survey of the current progress in the asymptotic description of the inherent hydraulic jump. Here also the recent and partially analogous results in [11] deserve a mention, of course.

2 Radially Spreading Thin Film

By (2), the bulk of the slender falling jet remains inviscid so that it is described by classical inviscid-flow theory. Due to the negligibly small capillary pressure according to (1e), Bernoulli's theorem yields $(u^2+w^2)/2-\bar{g}(d-z)\sim B(\psi)$ with the Bernoulli function $B(\psi)$ specified via (11a) and $\bar{g}:=gd$. The appealing idea of controlling the radially spreading thin film (in industrial applications) by controlling the imposed vorticity $B'(\psi)$ via a targeted design of the nozzle shape suggests to prevent the jet from being contracted markedly, according to Toricelli's law, and essentially unaffected by the specific form of w_o at its impingement. Hence, $\bar{g}$ should not be to large. We therefore stipulate a least-degenerate limit: $\bar{g}=O(1)$.

Prescribing a downstream condition consistent with the global flow picture and thus allowing for strict forward flow as $r\gg 1$ closes the problem of an inviscid free jet and its deflection where $z=O(r)$. From (3), $w/u\ll 1$ in the far field, which implies $u\sim\sqrt{2(B+\bar{g})}$ where ψ takes on similarity form: say, $\psi\sim f(\eta)/2$ with $\eta:=z/h(r)=O(1)$, thus $u\sim f'(\eta)/(2rh)$. Finally, by solving

$$f'=C\sqrt{2[B(f/2)+\bar{g}]},\quad f(0)=0,\quad f(1)=1,\quad 2rh\sim C=const, \tag{12}$$

we determine f and the eigenvalue C governing the radial flattening of the layer. Two model cases, i.e. of zero and constant vorticity, are of specific importance: (i) the irrotational (uniform) flow just beneath the nozzle exit, $w_o=-1$, yielding $B\equiv 1/2$, $f=\eta$ as $C=1/\sqrt{1+2\bar{g}}$; (ii) the classical (and more realistic) Hagen–Poiseuille profile $w_o=2(r^2-1)$, giving $B=2-4\psi$, $f=\sqrt{4+2\bar{g}}C(\eta-\eta^2)+\eta^2$, $C=\sqrt{1+\bar{g}/2}-\sqrt{\bar{g}/2}$. In [7], jet bending is accounted for more complex representations of w_o under the variation of $\bar{g}$ and jet contraction, even affected by capillarity.

Viscous boundary layers (BLs) form along the free surface and on the disc encompassing its centre. The second type merges with the predominantly inviscid flow considered above to eventually form the developed thin film spreading outwards. As long as submerged in the region of jet deflection, this rotory BL flow is parametrised by α_0 and exhibits a radial component matching that of the inviscid flow on its top. This accelerates from being of $O(r)$ near stagnation to $O(1)$. The following order-of-magnitude estimates give an account of the aforementioned merge, where ν serves as the basic perturbation parameter. At first, (3) and (4) entail

$$urh \sim 1, \quad u^2/r \sim \nu u/h^2 \tag{13a–c}$$

for the whole developed layer; (4) and (5) with (7c)

$$u^2/r \sim v^2/r \sim \nu u/\delta_K^2, \quad v \sim r\sqrt{\alpha_0}, \quad \delta_K := \nu^{1/2}\alpha_0^{-1/4} \tag{14a–c}$$

for a BL with thickness δ_K where rotation is dominantly at play (generalisation of the classical self-preserving von-Kármán-type BL underneath a stagnant flow, see [9]). We now advantageously consider three flow regimes.

(I) $r \sim r_\nu := \nu^{-1/3}$: there the dominant effect of viscous shear extends to the whole layer as long as rotation is so weak that $u \sim 1$ (from (13) with $u \sim 1$).

(II) $r \sim r_c := 1/\sqrt{\alpha_0}$: there the centrifugal force induces a u-component of $O(1)$ in the BL (from (14b) and $u \sim v \sim r\sqrt{\alpha_0}$).

(III) $r \sim r_r := \alpha_0^{-1/8}\nu^{-1/4}$: there the effect of rotation becomes important across the entire layer (from (13a) and (14) for $\delta_K \sim h$).

From this the useful categorisation (A)–(D) ensues, differing by the magnitude of r where rotation becomes effective:

(A) $\alpha_0 \ll \nu^{2/3}$, $(r_c \gg)\ r_r \gg r_\nu$ (*slowly rotating* film): relatively far downstream of the formation of a developed film.

(B) $\alpha_0 \sim \nu^{2/3}$, $r_c \sim r_r \sim r_\nu$ (*moderately rotating* film): where the developed film emerges (least-degenerate case).

(C) $\alpha_0 \gg \nu^{2/3}$, $r_c \ll r_r\ (\ll r_\nu)$ (*rapidly rotating* film): where the BL is still much thinner than the film. That is, the BL evolves towards a von-Kármán BL ($u \sim v \gg 1$) that has entrained the whole film for $r \sim r_r$.

(D) $1 \ll \alpha_0 \ll \nu^{-2}$ (*very rapidly rotating* film): according to (14b), the BL has already assumed von-Kármán form beneath jet impingement.

Finally, if r_r becomes of $O(1)$, i.e. α as large as ν^{-2}, the BL rotates so fast that it already sucks in the impinging jet and prevents it from being deflected in an essentially inviscid fashion. This scenario renders the current flow description invalid.

As suggested by the generic case (B) and item (II), we scrutinise the regime of competing inertial, centrifugal, and viscous forces, characterised by the coordinate stretching $(R,Z) := (\nu^{1/3}r, 2\nu^{-1/3}z) = O(1)$. Accordingly, we introduce the similarity parameter $\alpha := \nu^{-2/3}\alpha_0 = O(1)$, so that the flow regimes (A)–(D) and the associated terminology are readily identified below. Substituting the appropriate expansions $[\psi,u,v,w] \sim [\Psi/2, U, \alpha RV, \nu^{-2/3}W](R,Z)$, $h \sim \nu^{1/3}H(R)/2$ into (3)–(6) shows that the rescaled flow quantities satisfy a parabolic shallow-water problem as pressure forces remain negligibly small. This governs perfectly supercritical flow controlled by α and the vorticity introduced by the jet:

$$R[U,W] = [\Psi_Z, -\Psi_R], \tag{15}$$

$$UU_R + WU_Z - \alpha RV^2 = U_{ZZ}, \tag{16}$$

$$UV_R + WV_Z + 2UV/R = V_{ZZ} \tag{17}$$

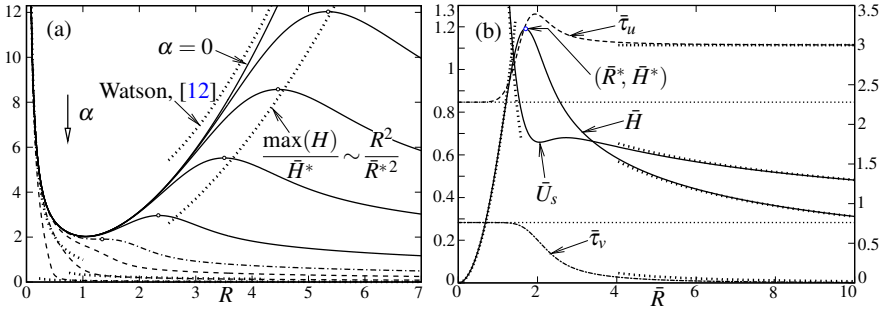

Fig. 2 Numerical solutions for strictly supercritical flow; *dotted* asymptotes refer to Watson's self-preserving flow, inviscid jet bending ($H \sim C/R$), and fully developed flow, cf. (22): (a) H vs. R, *solid*: $\sqrt{\alpha} = 0$, 0.01, 0.02, 0.05, 0.2, *dash-dotted*: $\sqrt{\alpha} = 0.723$, *dashed*: $\sqrt{\alpha} = 2$, 10, 100; (b) $\bar{H}$, $\bar{U}_s$ (left ordinate) and $\bar{\tau}_u$, $\bar{\tau}_v$ (right ordinate) vs. $\bar{R}$: canonical representations for slowly rotating flow

are supplemented with BCs given by (7b–d) and the leading-order forms of (8), (9) and ICs capturing the overlap of the thin-film region with that of inviscid jet deflection;

$$Z = 0\colon\ \Psi = U = 0,\ V = 1, \quad Z = H(R)\colon\ \Psi = 1,\ U_Z = V_Z = 0, \tag{18}$$

$$R \to 0\colon\ [U,V,H] \sim [f'(\zeta)\,\mathrm{sgn}(\zeta), 1-\mathrm{sgn}(\zeta), C/R],\ \ \zeta := Z/H(R). \tag{19}$$

By the absence of an upstream influence, a downstream condition as (11c) is ignored, i.e. the disc considered as infinitely large. Adopting an advanced Keller–Box scheme and advantageously utilising the coordinates R, ζ for marching downstream achieves highly accurate numerical solutions of (15)–(19). However, the ICs complying with the no-slip conditions in (18) render the problem singular, and its regularisation involves the BL structure discussed above. This is recovered for $R \to 0$ but itself becomes singular and splits into several flow regions in the limit $\alpha \to \infty$. In agreement with the scenarios (C) and (D), its full resolution involves the subtleties of matching exponentially varying terms (under investigation). In our numerical solutions for situation (i) with $\bar{g} \to 0$ above, an adaptive refining of the discretisation introduces the BL in an automated way. (This strategy and hence the numerical resolution for $R \ll 1$ are obviously compromised for rather large values of α.)

Equation (16) decouples from (17) for vanishingly small disc spin ($\alpha \to 0$). In the case $\alpha = v \equiv 0$ the subsequent analysis bears substantial analogies to but differs in subtle details from its counterpart applied to a planar layer; cf. [2, 4, 7]. These originate in the radial divergence of the flow, solely expressed by the factors r in (3).

As confirmed by Fig. 2(a), for rather high disc spin, the radially increasing centrifugal force accelerates the film flow throughout. If α is lowered, here if $\sqrt{\alpha}$ falls below $\simeq 0.723$, the viscous shear force first decelerates flow before the centrifugal one takes over. Hence, as a remarkable feature of the flow, H then undergoes a maximum. This becomes more pronounced and shifted outwards the lower the disc spin is. Eventually, for zero disc spin, Watson's classical self-similar flow, see

[12], is attained quite rapidly. This predicts an unbounded increase of the layer: $H/R^2 \to \bar{C} := \pi/(3\sqrt{3}) \simeq 0.6046$ ($R \to \infty$). In the limit $\alpha \to 0$, we restore (15)–(18) in full to leading order when we put a hat on all quantities therein and α set to unity as we consider the following expansion referring to a slowly rotating film,

$$[\Psi, U, V, W, H] \sim \left[\bar{\Psi}, \alpha^{3/8}\bar{U}, \bar{V}, \alpha^{1/4}\bar{W}, \alpha^{-1/4}\bar{H}\right], \quad \left(\bar{R}, \bar{Z}\right) := \left(\alpha^{1/8}R, \alpha^{1/4}Z\right). \tag{20}$$

Then generic conditions of matching with Watson's flow far upstream replace (19);

$$\bar{R} \to 0\colon \quad [\bar{\Psi}, \bar{V}, \bar{H}] \sim \left[f_W(\bar{\zeta}), g_W(\bar{\zeta}), \bar{C}\bar{R}^2\right], \quad \zeta := \bar{Z}/\bar{H}(\bar{R}), \tag{21}$$

with f_W, g_W denoting Watson's self-similar solution and the raised azimuthal component, governed by (16) for $\alpha = 0$ and (17). Consequently, this modification of the above problem describes the spread of the rotating film in universal form.

For its numerical solution, where $\bar{R}$, $\bar{\zeta}$ serve as independent variables, we refer to Fig. 2(b): $[\bar{\tau}_u, \bar{\tau}_v] := [\bar{\Psi}_{\bar{\zeta}\bar{\zeta}}, -\bar{V}_{\bar{\zeta}}](\bar{R}, 0)$ are the suitably scaled wall shear stresses; $\bar{U}_s$ is the surface speed $\bar{U}(\bar{R}, \bar{H})$; the height maximum occurs for $(\bar{R}, \bar{H}) = (\bar{R}^*, \bar{H}^*) \simeq (1.700, 1.191)$, confirmed for even rather moderate values of α; see Fig. 2a.

By viscous diffusion, the predominant centrifugal–shear balance for large values of $\bar{R}$ drives the flow towards its fully developed terminal state where the fluid rotates like a solid body ($\bar{V} \sim 1$), as spotted in Fig. 2. One finds that

$$\left[\bar{U}\bar{R}^{1/3}, \bar{R}^{8/3}(\bar{V} - 1), \bar{H}\bar{R}^{2/3}\right] \sim 3^{1/3}\left[3^{1/3}(\bar{\zeta} - \bar{\zeta}^2/2), -2\bar{\zeta} + \bar{\zeta}^3 - \bar{\zeta}^4/4, 1\right], \tag{22}$$

where the reminder term is a power series in $\bar{R}^{-8/3}$. This entails the similarity laws $UR^{1/3} = O(\alpha^{1/3})$ and $HR^{2/3} \sim (3/\alpha)^{1/3}$ at play for $R \gg \alpha^{-1/8}$, hence $U \ll \alpha^{3/8}$ and $H \ll \alpha^{-1/4}$. These relationships state $r \gg r_r$, $u \ll r_r\sqrt{\alpha_0}$, $h \ll \delta_K$, according to (III) and (14b,c) above. Then scenario (C) ensures their validity far downstream from film formation for very large values of α. In that case, the von-Kármán BL comprises the whole layer and avoids the formation of its height maximum. During its evolution, the accordingly overshooting U-profiles are gradually transformed into the parabolic one predicted by (22).

The otherwise negligibly weak streamline curvature due to plate-normal momentum transfer and possibly its interplay with the capillary and hydrostatic pressure variations, see (6), perturb the current flow structure by virtue of a strong viscous–inviscid interaction emerging near the real disc edge ($r = r_e$). This accomplishes the gradual transition from the no- to a free-slip condition, cf. [8]. Inspection of (6) and (4) discloses that the associated upstream effect leads to a global failure of the above structure once h has increased such that gh has become of $O(u^2)$ and the developed liquid layer undergoes a viscous hydraulic jump.

3 Upstream Influence: The Toroidal Viscous Hydraulic Jump

In classical hydraulic engineering, the occurrence of the hydraulic jump is referred to a discontinuity separating two states of an inviscid flow in the shallow-water limit, i.e. with the pressure being hydrostatic; see [10]. Thus, the irreversible energetic losses are first construed as being concentrated in the infinitesimally thin interface. This, at a first glance obvious idealisation has led to some fundamental insight and to the celebrated analogy to inviscid gas dynamics, with the Froude number taking the place of the Mach number and the jump that of a shock wave. However, as a closer look shows, it suffers from the severe conceptional shortcoming that shocks manifest exact weak solutions of the Euler equations whereas here their contraction process provokes an unbounded growth of the wall-normal flow component, violating the initially quasi-one-dimensional approach. Therefore, a rational treatment of the jump phenomenon recognises the typical sudden increase of the elevation of the layer as inevitably smeared ("bore") over a finite distance, accounting for its dissipative structure and vanishing if the Reynolds number grows beyond all bounds. The complete description of a marginally weak (transcritical) hydraulic jump within this asymptotic framework of triple-deck theory, namely as an eigensolution settling in a nonlinear fashion essentially by an interplay of gravity and viscous forces only dominant in a thin sublayer adjacent to the wall, was first accomplished in [5].

3.1 The Weakly Elliptic Problem

As a consequence of the aforesaid, in the current setting governed by (1) and (A)–(D) in Sect. 2, the viscous hydraulic "jump" can arise for slowly rotating developed flow. It thus typifies a smooth solution of the shallow-water problem including the hydrostatic pressure gradient on the global characteristic length, the disc radius r_e.

In order to extend the above canonical flow representation for $\alpha_0 \ll \nu^{2/3}$ towards both the case of zero disc spin and the inclusion of the pressure gradient, we formally replace α in (20) by some small perturbation parameter β. With the aid of (6) and (10) and the previous transformations between the original variables and the current ones, this entails the following generalisation of (16):

$$\bar{U}\bar{U}_{\bar{R}} + \bar{W}\bar{U}_{\bar{Z}} - \bar{\alpha}\bar{R}\bar{V}^2 = \bar{U}_{\bar{Z}\bar{Z}} - \bar{P}'(\bar{R}), \quad \bar{P}(\bar{R}) := G\bar{H} - S\bar{H}'', \tag{23}$$

$$\bar{\alpha} := \alpha/\beta, \;\; G := g\nu^{1/3}/(2\beta), \;\; S := \sigma\nu/(2\beta^{3/4}), \;\; \bar{R} \le \bar{R}_e := r_e\nu^{1/3}\beta^{1/8}. \tag{24}$$

For physically realistic flows, it is expedient to assume $S \ll G$. (However, capillarity can be at play to leading order as streamline curvature and correspondingly drastic changes of $\bar{H}$ render the shallow-water approximation invalid near the disc edge; cf. [8].) We consider a least-degenerate distiguished limit by taking the remaining parameters $\bar{\alpha}$, G, $\bar{R}_e$ as of $O(1)$, where the rescaled disc radius $\bar{R}_e$ controls the inevitable upstream influence if $G > 0$ in an awkward manner elucidated below. Then (23) supplemented with (15), (23), (17), (18), and (21) (overbars added) gov-

erns the viscous hydraulic jump. Notably, the film height steepens more abruptly as the typical Froude number $1/G$ becomes smaller. The associated onset of the jump was first appreciated rigorously in [2]; the global structure for its two-dimensional counterpart in [4]. Here some novel insight, tied in with disc rotation, is put forward.

There are three sensible possibilities to define β in (24):

(a) $\beta := \alpha$ means a pronounced hydrostatic effect by the increased film height if $G = O(1)$ or $g = O(\alpha_0/\nu)$;
(b) $\beta := g\nu^{1/3}/(2G)$, $G = const$ measures the impact of rotation on the jump;
(c) $\beta := r_e^{-8}\nu^{-8/3}$ or $\bar{R}_e = 1$ as the most obvious, physically motivated, choice, morphing the original scaling given by the nozzle flow into $\bar{\alpha} = \bar{\alpha}_c := \alpha_0 r_e^8 \nu^2$, $G = G_c := g r_e^8 \nu^3/2$, $S = S_c := \sigma r_e^6 \nu^3/2$ (r_e is the characteristic lenght scale).

The choices (a) and (b) resort to the dominant parabolic structure of the problem and make evident that a viscous jump can only be expected if r_e is not much smaller than r_r, according to the items (III) and (A) in Sect. 2, or $g^{-1/8}\nu^{-3/8}$.

Inspection of (23) for $G > 0$ shows that the marching problem ignoring a downstream condition is ill-posed as a scale shortening arising for $\bar{R} \to 0$ causes the emergence of a sublayer where $\bar{\zeta} = O(G\bar{R}^{8/3})$ and convection, pressure and viscous shear predominate. In turn, irregular expansions of strong superexponential variations superimpose the regular ones controlled by Watson's solution. For instance,

$$\frac{\bar{H}}{\bar{C}\bar{R}^2} \sim 1 + \bar{R}^8\Big[A\exp\Big(-\frac{\Omega}{G^3\bar{R}^{24}}\Big) + O(1)\Big], \quad \Omega := \frac{3^{17/2}}{2^8\pi^{15/2}}\frac{\Gamma(\frac{1}{3})^{12}}{\Gamma(\frac{5}{6})^{15}} \simeq 184.094\,. \tag{25}$$

Herein, positive/negative values of the constant A, presently determined by the resolution of our marching scheme, refer to a compressive/expansive branch-off from Watson's self-preserving flow. This inevitably has our marching solutions terminate at some $\bar{R} = \bar{R}_t$, say, in the form of the universal singularity of expansive type discussed extensively in [4]. However, as the associated scale shortening must initiate the aforementioned invalidity of the shallow-water approximation, $\bar{R}_t$ is identified with $\bar{R}_e$ and thus fixes the value of A. Most important, h_e in (11c) can *not* be prescribed but is part of the solution as that singularity is to be met at $\bar{R} = \bar{R}_e$. Hence, a compressive bifurcation having a strength A parametrised by α, G, and $\bar{R}_e$ such that the flow re-expands as $\bar{R} \to \bar{R}_e$ effects the jump. This subtle intrinsic ellipticity or upstream influence generated at the plate edge unequivocally settles the known existing controversies on its position and strength and accompanying flow separation.

The marching procedure for tracking the bifurcation is computationally much less expensive than iterative elliptic schemes including the singularity (as a transient one, see [4]). Efforts are under way to implement (25), allowing for a proper control of A such that a jump indeed forms. Also, the transformation invariance of (23) enables a (preliminary) systematic study; the subscripts c indicate item (c), see Fig. 3:

$$[\bar{R}, \bar{Z}, \bar{H}, \bar{U}, \bar{\alpha}, G] = \big[\bar{R}_e\bar{R}_c, \bar{R}_e^2\bar{Z}_c, \bar{R}_e^2\bar{H}_c, \bar{U}_c/\bar{R}_e^3, \bar{\alpha}_c/\bar{R}_e^8, G_c/\bar{R}_e^7\big]. \tag{26}$$

Viscous diffusion can facilitate a lubrication limit of (23) governed by the order-of-magnitude estimates $\bar{U}\bar{R}\bar{H} \sim 1$, see (13a), $\bar{V} \sim 1$, $\bar{U}^2/\bar{R} \ll G\bar{H}/\bar{R} \sim \bar{\alpha}\bar{R} \sim \bar{U}/\bar{H}^2$.

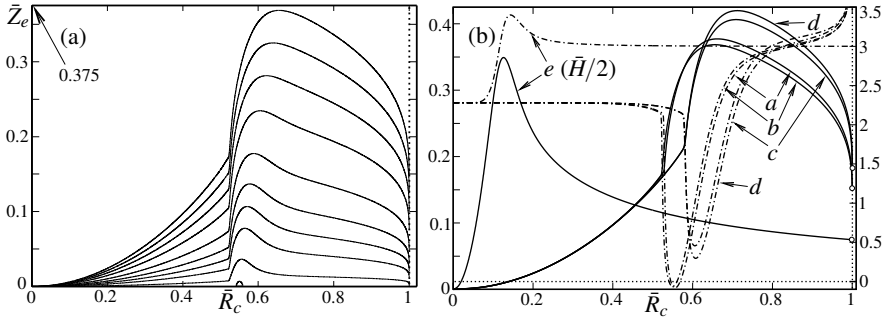

Fig. 3 Jumps by (25): (a) $(G,\bar{\alpha},\bar{R}_e)=(1,0.027,\simeq 2.008)$, $(\bar{\alpha}_c,G_c)\simeq(7.145,131.77)$, $\bar{\Psi}=0$ (encircling separation bubble), 0.002, 0.02, 0.05, 0.1, 0.2, 0.4, 0.6, 0.8, 1; (b) $\bar{H}_c$, $\bar{\tau}_u$ as in Fig. 2(b), *a*: $(G,\bar{\alpha},\bar{R}_e)=(1,0,\simeq 1.985)$, *b*: see (a), *c*: $(2,0.5,\simeq 1.694)$, *d*: $(8,2,\simeq 1.413)$, *e*: $(1,9,10)$ (regular)

Then $\bar{R}\gg\bar{H}^{1/2}$, i.e. also $\bar{R}\gg\bar{\alpha}^{-1/8}$ and $G\gg\bar{\alpha}$ from integration of (23) subject to (18):

$$\bar{U}\sim\frac{3\bar{\alpha}^{1/2}}{G^{1/8}\hat{R}\hat{H}}\Big(\bar{\zeta}-\frac{\bar{\zeta}^2}{2}\Big),\quad \hat{R}-\frac{\mathrm{d}\hat{H}}{\mathrm{d}\hat{R}}=\frac{3}{\hat{R}\hat{H}^3},\quad \big(\hat{R},\hat{H}\big):=\Big(\frac{\bar{\alpha}^{1/2}}{G^{3/8}}\bar{R},G^{1/4}\bar{H}\Big).\quad(27)$$

Hence, $\hat{H}'(\hat{R})<0$, $\hat{H}^4\sim-12\ln\hat{R}$ in the gravity-dominated upstream limit $\hat{R}\to 0$, which is also discerned for $G\ll 1$ and $\bar{R}=O(1)$, cf. [4], and $\hat{H}\sim(3/\bar{R}^2)^{1/3}$ in the rotation-controlled downstream limit $\hat{R}\to\infty$ of fully developed flow, see (22). As the first cannot be maintained for arbitrarily large values of $\hat{R}$, either the expansive singularity terminates downstream marching or the centrifugal force enters the lubrication approximation further downstream: increased disc rotation diminishes the jump strength and finally suppresses the edge singularity, as the result in Fig. 3(b) for $G=1$, $\bar{\alpha}=9$ confirms and is currently studied in full depth and breadth.

3.2 On the Role of Surface Tension

We multiply (23) with $\bar{R}\bar{U}$, conveniently add $\bar{R}\bar{W}\bar{P}_{\bar{Z}}\equiv 0$, and integrate the so obtained equation over some fraction $\mathscr{V}$ of the whole layer bounded by vertical up- and downstream sections at $\bar{R}=\bar{R}_u$ and $\bar{R}=\bar{R}_d$ $(>\bar{R}_u)$, say. With (15) and the aid of the divergence theorem and a "jump" operator applied to some quantity $Q(\bar{R},\bar{Z})$,

$$[\![Q]\!]:=\bar{R}_d\int_0^{\bar{H}(\bar{R}_d)}Q(\bar{R}_d,\bar{Z})\,\mathrm{d}Z-\bar{R}_u\int_0^{\bar{H}(\bar{R}_u)}Q(\bar{R}_u,\bar{Z})\,\mathrm{d}\bar{Z},\qquad(28)$$

we recover the shallow-water approximation of the mechanical-power budget for $\mathscr{V}$,

$$\tfrac{1}{2}\big[\![\bar{U}^3]\!\big]+G\big[\![\bar{H}]\!\big]-S\big[\![\bar{H}''\big]\!\big]=\int_{\bar{R}_u}^{\bar{R}_d}\int_0^{\bar{H}(\bar{R})}\big(\bar{U}\bar{V}^2-\bar{R}\bar{U}_{\bar{Z}}^2\big)\,\mathrm{d}\bar{Z}\,\mathrm{d}\bar{R}\qquad(29)$$

as $[\![\bar{U}\bar{R}\bar{U}]\!] = 0$; see (13a): the net flux of the inertial (kinetic and potential) energy as well as the capillary pressure through the confining cross-sections equals the power exerted by the centrifugal (body) force and the negative viscous dissipation in $\mathscr{V}$.

Notably, as seen from the derivation of (29), surface tension *has no impact* on the conversion of mechanical energy under the absence of the Marangoni effect and the associated tangential surface stress. Here the following rationale is illuminating. To this end, we for the moment relax a basic assumption by allowing $S = S(\bar{R})$, i.e. for the Marangoni effect. Then $S'(\bar{R})$ equals the thereby generated Marangoni stress, τ_M, exerted in radial direction on the liquid just below the surface. Multiplying this tangential stress equilibrium for an infinitesimally short surface filament in the shallow-water limit with the surface speed $\bar{U}_s$ yields upon integration by parts

$$(S\bar{U}_s)(\bar{R}_u) - (S\bar{U}_s)(\bar{R}_d) - \int_{\bar{R}_u}^{\bar{R}_d} \bar{U}_s S' \mathrm{d}\bar{R} = M := \int_{\bar{R}_u}^{\bar{R}_d} \tau_M \,\mathrm{d}\bar{R}. \tag{30}$$

This relationship states that the powers of externally (first two contributions and $-M$) and internally (third term) acting stresses add up to zero for an infinitesimally thin control cell $\mathscr{C}$ encompassing the considered fraction of the inertia-less free surface, in full agreement with the conventional statement about the conservation of mechanical energy. Conversely, if the control volume $\mathscr{V}$ just excludes $\mathscr{C}$, one would have to add M on the right-hand side of (29) (the capillary pressure acting onto the surface is powerless). Adding this and (30) recombines these two control cells to the original one, $\mathscr{V}$: since the surface powers M and $-M$ cancel, (29) is recovered with the first three terms in (30) added on its right-hand side. Accordingly, these denote the externally and internally effected powers of surface tension. By (30), these sum up to M, thus furnishing the correct extension of (29) if $S' = \tau_M \not\equiv 0$.

Unfortunately, these quite basic findings have apparently been confounded in the very recent (intensely debated) study [1]. The mechanical-power balance therein, see Eq. (5.2) in [1], contains erroneously (amongst other doubtful terms) the external power of surface tension, of $O(\sigma ur)$. Its difference, giving the first two terms in (30), is referred to as "the increase of the surface area". In fact, the cancelling third term in (30) describes the stretching of the surface due to the infinitesimally small relative speed $\bar{U}_s(\bar{R}+\mathrm{d}\bar{R}) - \bar{U}_s(\bar{R})$ of neighbouring fluid particles. However, the power balance in [1] lacks this and the capillary contributions to (29). The latter are of $O(\sigma urhh'')$ (where (13a) holds). This discloses the queried appearance of the external capillary power as inconsistent with the underlying slender-layer approximation or $|h''| \ll 1$, in [1] postulated tacitly (and unquestioned) even when the control volume is radially contracted. In our opinion, the hydrostatic contributions of $O(gurh^2)$, see (29), then misled the authors of [1] to their central statement, namely that the local Weber number $We := u^2h/\sigma$ balances the local Froude number $Fr := u^2/(gh)$ in leading order, obviously in conflict with the correct estimate $\sigma h'' \sim gh$ or $We/Fr \sim |h''| \ll 1$ expressing a hydrostatic–capillary force balance; cf. [3]. Therefore, the authors' novel assertion that "hydraulic jumps result form energy loss due to surface tension" where "gravity plays no significant role" and their

associated interpretation of the (admittedly, intriguing) experimental findings must be questioned seriously in the light of their incorrect adoption of the energy balance.

4 Further Outlook

It is the ultimate goal of an advanced asymptotic theory to clarify the transition of the flow passing the edge towards a developed downfall parabola for $G = O(1)$, which completes the overall picture of the viscous hydraulic jump and is topic of our ongoing research. So far, this task has been accomplished partially under the assumption $G \ll 1$, namely when the effect of streamline curvature by disc-normal momentum transfer dominates locally over the gravitational one; see [8]. The rational description of the free-surface eddy or "roller" emerging during the hydraulic jump for sufficiently small Weber numbers immediately upstream of separation—and observed experimentally, but in [4] also numerically by an *ad-hoc* inclusion of streamline curvature into the classical shallow-water problem—attracts particular interest. Once the laminar hydraulic jump is fully understood under a variation of the Froude and Weber numbers, the laminar–turbulent transition accompanying it provides a most formidable challenge to be mastered with asymptotic techniques.

Acknowledgements The author is grateful to the Austrian Research Promotion Agency (FFG) for granting this research within the *COMET K2* programme (grant no.: 849109, project acronym: *XTribology*).

References

1. Bhagat, R.K., Jha, N.K., Linden, P.F., Wilson, D.I.: On the origin of the circular hydraulic jump in a thin liquid film. J. Fluid Mech. **851**, R5-1–R5-11 (2018), https://doi.org//10.1017/jfm.2018.558
2. Bowles, R.I., Smith, F.T.: The standing hydraulic jump: theory, computations and comparisons with experiments. J. Fluid Mech. **242**, 145–168 (1992), https://doi.org/10.1017/s0022112092002313
3. Bush, J.W.M., Aristoff, J.M.: The influence of surface tension on the circular hydraulic jump. J. Fluid Mech. **489**, 229–238 (2013), https://doi.org/10.1017/S0022112003005159
4. Higuera, F.J.: The hydraulic jump in a viscous laminar flow. J. Fluid Mech. **274**, 69–92 (1994), https://doi.org/10.1017/s0022112094002041
5. Kluwick, A., Cox, E.A., Exner, A., Grinschgl, Ch.: On the internal structure of weakly nonlinear bores in laminar high Reynolds number flow. Acta Mech. **210** (1–2), 135–157 (2010), https://doi.org/10.1007/s00707-009-0188-x
6. Martens, E.A., Watanabe, S., Bohr, T.: Model for polygonal hydraulic jumps. Phys. Rev. E **85** (3), 036316-1–036316-14 (2012), https://doi.org/10.1103/PhysRevE.85.036316
7. Scheichl, B., Kluwick, A.: Laminar spread of a circular liquid jet impinging axially on a rotating disc. J. Fluid Mech. **864**, 449–489 (2019), https://doi.org//10.1017/jfm.2018.1009
8. Scheichl, B., Bowles, R.I., Pasias, G.: Developed liquid film passing a trailing edge under the action of gravity and capillarity. J. Fluid Mech. **850**, 924–953 (2018), https://doi.org/10.1017/jfm.2018.464

9. Tifford, A.N. & Chu, S.T.: On the flow around a rotating disk in a uniform stream. J. Aeron. Sci. **19** (4), 284–285 (1952), https://doi.org/10.2514/8.2255
10. Valiani, A., Caleffi, V.: Free surface axially symmetric flows and radial hydraulic jumps (Technical Note). J. Hydraul. Eng. **142** (4), 06015025-1–06015025-6 (2016), https://doi.org/10.1061/(ASCE)HY.1943-7900.0001104
11. Wang, Y., Khayat, R.E.: Impinging jet flow and hydraulic jump on a rotating disk. J. Fluid Mech. **839**, 525–560 (2018), https://doi.org/10.1017/jfm.2018.43
12. Watson, E.J.: The radial spread of a liquid jet over a horizontal plane. J. Fluid Mech. **20** (3), 481–499 (1964), https://doi.org/10.1017/S0022112064001367